

Intermittent dynamics in complex systems driven to extinction

Juan V Escobar^{1,*} & Isaac Pérez Castillo^{2,3}

¹*Instituto de Física, Universidad Nacional Autónoma de México. Apdo. Postal 20-364, Cd. Mx., Mexico, C.P. 04510*

²*Departamento de Cuántica y Fotónica, Instituto de Física, Universidad Nacional Autónoma de México. Apdo. Postal 20-364, Cd. Mx., Mexico, C.P. 04510*

³*London Mathematical Laboratory, 14 Buckingham Street, London WC2N 6DF, United Kingdom*

When complex systems are driven to extinction by some external factor, their non-stationary dynamics can present an intermittent behaviour between relative tranquility and burst of activity whose consequences are often catastrophic. To understand and ultimately be able to predict such dynamics, we propose an underlying mechanism based on sharp thresholds of a local generalized energy density that naturally leads to negative feedback. We find a transition from a continuous regime to an intermittent one, in which avalanches can be predicted despite the stochastic nature of the process. This model may have applications in many natural and social complex systems where a rapid depletion of resources or generalized energy drives the dynamics. In particular, we show how this model accurately describes the time evolution and avalanches present in a real social system.

Avalanches or bursts of activity are present in many natural and social systems that range from sand piles¹, earthquakes², solar flares³, plastic deformation⁴, domain flips in ferromagnets⁵,

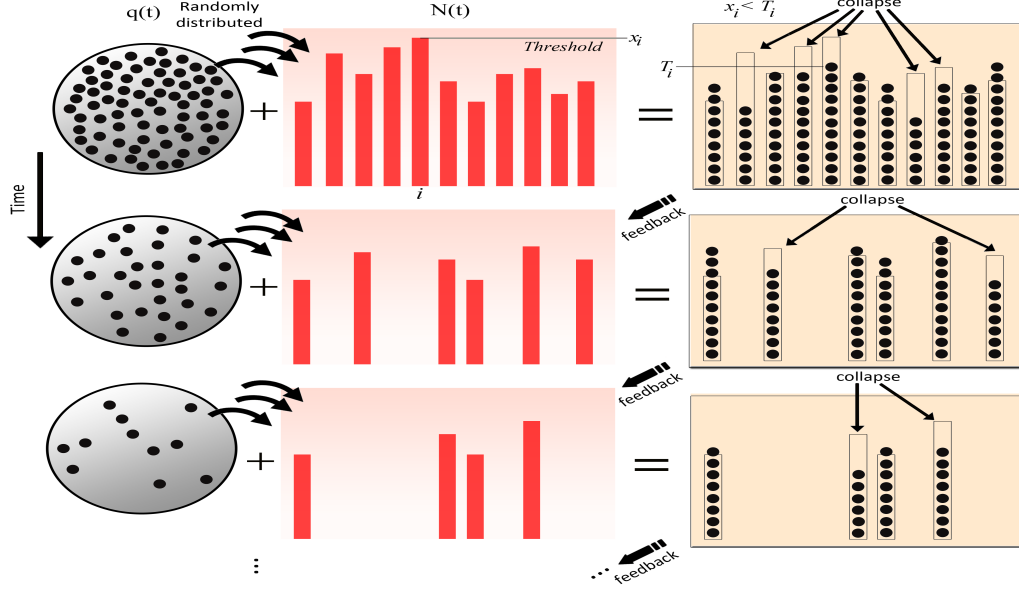


Figure 1: Schematic diagram of the negative feedback mechanism proposed: A decaying input signal $q(t)$ is randomly distributed at time t among $N(t)$ elements. When $T_i(t)$ crosses a threshold x_i , element i becomes inactive, thus decreasing the overall number of active elements $N(t)$.

species mass extinctions⁶, neuronal activity⁷, forest fires⁸, landslides⁹, clustering of self driven particles¹⁰ and hydrodynamics¹¹, to daily website hits¹², attendance to motion pictures¹³, financial markets¹⁴ and book sales¹⁵. Understanding and ultimately predicting the dynamics of these avalanches is of great scientific and practical importance, as they can lead to catastrophic events, of which large earthquakes and stock market crashes serve as two dramatic examples.

A very fruitful approach to understand the dynamics of many of these systems has been to assume local and relatively simple interactions of their constituting elements which drive the system to a state that displays emergent behaviour. Importantly, this emergence results without

the need of an external tuning parameter^{16,17}. This is the premise of Self Organized Criticality (SOC)¹, for which models now abound. A paradigmatic example is that of earthquakes, which may be modelled as dissipative systems presenting SOC^{18,19}. There, a slow energy input eventually leads to relatively fast breakdown events spanning many orders of magnitude. Variations of this model²⁰, based on the Bak, Tang and Wiesenfeld (BTW) sand-pile model²¹, are able to recover the main characteristics of earthquakes statistics. Roughly speaking, this class of BTW models have two main ingredients. First, there is a continuous input of energy into the system that may continue indefinitely. Second, bursts of activity occur due to excess stress accumulation which is then toppled to neighbouring constituents giving rise to avalanches.

There exist, however, a plethora of other systems which are instead characterized by a steady decrease of their activity all the way to complete inertness. This happens as a result of a steady decay of the input energy, which translates into the system as an effective stress to which it must adapt, reaching at every step a new equilibrium configuration. While in some instances this is achieved in a relatively smooth way, in others the system is unable to adapt fast enough giving rise to large, often catastrophic events. Indeed, one may see an intermittent behaviour between relative tranquility and bursts of activity. Actually, it is now recognized that continuous driving forces can induce transitions between continuous and intermittent dynamics²². This feature is of great importance, since systems that seem to be adapting well (smoothly) to such external stresses, may suddenly break down without any apparent warning signs. Examples of systems presenting this general behaviour range from the group of theaters showing a particular movie as weekly audience decreases, the number of surviving a mammalian genera during an extinction period or the price

of a stock during a sell-off.

To model this behaviour we consider a system of non-interacting elements that receive (but do not accumulate) a share of the energy externally provided. Each element is pre-assigned a sharp threshold such that if the energy it has received is below this threshold, the element is permanently removed from the system. We show below that this simple model naturally leads to a negative feedback responsible for the adaptation of the system as a whole. The general mechanism proposed is depicted in figure 1. This model reproduces both the smooth response as well as the intermittent one and provides a means of predicting catastrophic events in complex systems as they are driven to extinction. To be mathematically precise, our model consists of N basic elements labelled with $i = 1, \dots, N$, a time-decaying external input signal $q(t)$, that for sake of clarity we assume it takes integer values, and a fixed set of thresholds $x_i > 0$ for each of the constituents $i = 1, \dots, N$ drawn randomly from a distribution. At a given time step t , each element can be either active or inactive, but once it has become inactive it remains in that state. Let $\sigma_i(t)$ be the state of element i , with $\sigma_i(t) = 0$ for the element being inactive, or one otherwise. If $N(t) = \sum_{i=1}^N \sigma_i(t)$ denotes the number of active elements at time t , the system evolves according to the following simple microscopic dynamical rule:

$$\sigma_i(t+1) = \sigma_i(t) \Theta(T_i(t) - x_i) . \quad (1)$$

Here $\Theta(x)$ represents the Heaviside step function, and $T_i(t)$ is a portion of the input signal uniformly and randomly allotted to active particle i such that $\sum_{i=1}^{N(t)} T_i(t) = q(t)$. Henceforth, we will call the set of variables $T_i(t)$ the occupancies. Notice that at a given time t , the probability of finding a particular configuration $\{T_1(t), \dots, T_{N(t)}(t)\}$ follows a multinomial distribution with

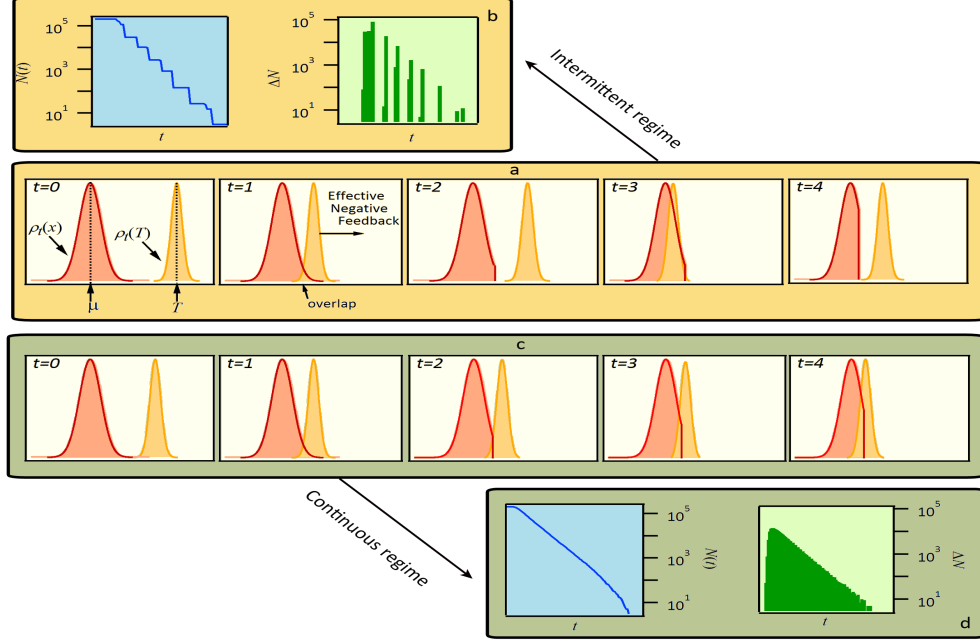


Figure 2: Schematics of the time evolution of the number of active elements $N(t)$, represented by their distribution of thresholds $\rho_t(x)$ (solid line) and of the distribution of occupancies $\rho_t(T)$ (dashed line), evidencing the negative feedback that takes place in a) the intermittent and c) the continuous regimes. The dynamics is described in the main text. The corresponding typical activities, $\Delta N(t)$, for each regime are shown in figures b) and d).

uniform probability $1/N(t)$. This implies that the average occupancy is the same for all elements and equal to $T(t) \equiv E[T_i] = q(t)/N(t)$, with variance being $\text{Var}[T_i(t)] = q(t)(1 - 1/N(t))/N(t)$. We take the initial conditions in which all constituents are active at $t = 0$, that is $N(t = 0) = N$, and define the activity for this model as the number of elements removed at each step $\Delta N(t) = N(t) - N(t + 1)$.

One can gain some intuition on how the system behaves under this mechanism by looking

at the time evolution of the density of active thresholds and the density of occupancies, denoted as $\rho_t(x)$ and $\rho_t(T)$ respectively. This will become useful to gain a good grasp on the mean-field solution to the model, presented below. Figure 2a shows a sketch of the dynamical evolution of the system in terms of these two densities. Let us assume that at a given time these two distributions do not overlap (Figure 2a, $t = 0$). Then, as time evolves, the distribution $\rho_t(T)$ moves to its left since the average occupancy $T(t) = q(t)/N(t)$ decreases over time, as $q(t)$ is a decreasing function and $N(t)$ has not changed yet. Eventually, the two distributions do overlap (Figure 2a, $t = 1$). This means that the overlapping fraction of active thresholds will become inactive, increasing the average occupancy $T(t)$, and pushing, in turn, the distribution $\rho_t(T)$ back towards higher values. As a consequence, a non-zero activity indirectly hinders any further activity, in what constitutes a negative feedback mechanism. Now again, the distributions are not overlapping (Figure 2a, $t = 2$) but, as time evolves, this mechanism reoccurs (Figure 2a at $t = 3$ and $t = 4$). This sequence of events repeats itself until all elements have become inactive. Since in this sequence the system goes through periods of zero activity, Figure 2a actually illustrates its typical response when it is in the herein called intermittent regime. But with this representation it is also possible to foresee that if the external signal decays relatively slowly, the system will be able to adapt to the depletion of resources, so that small but finite portions of $\rho_t(x)$ are removed at every iteration (Figure 2c). We call this the continuous regime since the activity is always non-zero. The different behaviour of the system in both regimes can be appreciated in the plots of $N(t)$ and $\Delta N(t)$ presented on Figures 2b and 2d for the intermittent and continuous regimes, respectively. These plots also help illustrate an important characteristic of the model: the maximum activity can be larger in the intermittent

regime by over an order of magnitude as compared to the continuous one.

At this point it is important to contrast our model with the BTW model, as both present avalanches and are based on a sharp threshold dynamics as a response to some external energy input. In the BTW model, the elements $q_i(t)$ may represent the accumulated stress allocated in one of the $N(t)$ geological faults, and, as in our model, an earthquake or avalanche occurs when a fault crosses its threshold. But, unlike our model in which the elements remain inactive once they are brought to that state, as soon as a geological fault has toppled its excess stress, it can start again accumulating new stress. Another important difference is that in the BTW model the input signal keeps providing energy which the system continuously dissipates, while, in our case, the input signals evolves in times towards zero. Furthermore, our model does not allow any stress accumulation; in other words, it is history independent. Indeed, despite their shared characteristics, the actual mechanism giving raise to bursts of activity in each model is completely opposite in nature: in the BTW model avalanches result from a positive feedback mechanism, while in ours, a negative feedback one plays the central role.

For concreteness, to quantify the behaviour of the model we have chosen an exponentially decaying external signal $q(t) = q_0 e^{-t/\tau}$ and proceeded to identify the continuous and intermittent regimes of the model in its space of parameters. As relevant parameters, apart of τ , we have also chosen the initial coefficient of variation $\kappa \equiv \sigma/\mu$ of the distribution of active thresholds $\rho_{t=0}(x)$, where μ and σ^2 are its first two cumulants. We have subsequently estimated the dynamical phase diagram corresponding to the the microscopic dynamics of equation (8) using two methods: i) by

deriving a simple dynamical mean-field equation and ii) by Monte Carlo simulations.

Even though it is possible to obtain an exact effective macroscopic dynamics using the method of the generating functional analysis a la Martin-Siggia-Rose²³, the resulting equations are rather cumbersome to analyse. Thus we have opted to derive a simpler dynamical mean-field equation, which turns out to describe the exact microscopic dynamics remarkably well. After some algebra, a dynamical mean-field equation for the average number of active elements, which we also denote as $N(t)$, is given by (see SI)

$$N(t+1) = \frac{N(t)}{2} \operatorname{erfc} \left(\frac{\mu - T(t)}{\sqrt{2(\sigma^2 + T(t))}} \right). \quad (2)$$

To identify in which regime the model is in the parameter space $(\kappa, 1/\tau)$, we introduce two order parameters. The first one is a natural way to quantify intermittency through the normalized cumulative time of inactivity (see SI). In particular, this quantity is 0 when the system is in the continuous regime, and non-zero when in the intermittent one. The second parameter characterizes the ability of the system to follow the input signal and corresponds to see whether $z(t) \equiv \frac{\mu - T(t)}{\sqrt{2(\sigma^2 + T(t))}}$ equals a constant z_* after some transient. By iterating the dynamical mean field equation (2) and following the values of these two parameters we are able to identify four regimes or phases in the $(\kappa, 1/\tau)$ -plane. Moreover, we are able to obtain analytical expressions for some of the transition lines. These four regimes are shown in Figure 3a. The intermittent regime, depicted in Figure 3a by a red filled area, is characterised by the impossibility of the system to synchronise with the external signal, resulting in avalanches. The continuous & asynchronous regime I (shown as the dark blue area in the same figure) corresponds to the system being again unable to synchronize to the external signal, but this time in a smooth way, *i.e.*, avalanches are no longer generated. On

the other side, in the continuous & synchronous regime, shown by the green area in Figure 3a, the system is able to follow the external signal. Finally, the continuous & synchronous regime II, captures the impossibility of the system to match the external signal due solely to restrictions in the initial conditions $T(t) > 0$.

Notice that, within the mean-field approximation, it is possible to obtain analytically the bifurcation line, denoted as $\kappa_c(\tau)$, separating the asynchronous to the synchronous regimes, as well as the bifurcation line $\kappa_{na}(\tau)$ separating the synchronous to the asynchronous regime II. The first line is derived by assuming that the synchronous regime is characterised by $z(t) = z_*$ being a constant. This implies, in turn, that z_* and τ are related by the formula $z_*(\tau) = \text{erfc}^{-1}(2e^{-1/\tau})$.

Naturally, the transition to the intermittent regime is derived by assuming a continuous bifurcation of $z(t)$ around z_* . After some algebra, the line separating both regimes in the $(\kappa, 1/\tau)$ -plane is given by the following set of coupled equations:

$$\begin{cases} e^{z_*^2} \text{erfc}(z_*) = \frac{(\mu + 2(\kappa\mu)^2 + T_*)T_*}{2\sqrt{2\pi}((\kappa\mu)^2 + T_*)^{3/2}} \\ z_*(\tau) = \frac{\mu - T_*}{\sqrt{2((\kappa\mu)^2 + T_*)}} \end{cases}, \quad (3)$$

with $\frac{1}{\tau} = -\log\left[\frac{\text{erfc}(z_*)}{2}\right]$. Thus, given μ , the solution of (8) results in a pair $(\kappa_c(\tau), T_*(\tau))$, where the first function $\kappa_c(\tau)$ corresponds to the bifurcation line separating the aforementioned regimes, while line $T_*(\tau)$ tells which value $T(t)$ takes precisely at the transition. As shown in Figure 3a, the agreement between the bifurcation line (8) and the dynamical phase diagram obtained from the same equation is excellent (see the SI for more details on the synchronization plots for this and other values of μ). The second bifurcation line, as reported in Figure 3a, follows from the fact

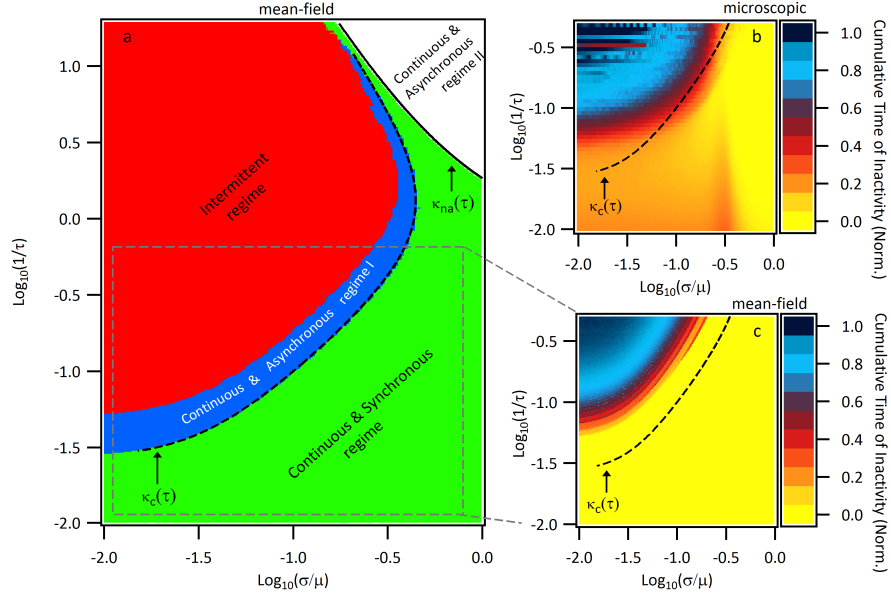


Figure 3: Analysis of dynamical phase-diagram. a) Phase diagram for the mean field model. Plots b) and c) show the intermittency phase diagram for the exact microscopic model and for the mean-field one, respectively. We also report the line $\kappa_{na}(\tau)$ in figure a) and the line $\kappa_c(\tau)$ in all plots. The Monte Carlo simulations were carried out by taking $q(0) = 2 \times 10^9$, $N(0) = 2 \times 10^5$, and $\mu = 1000$, and subsequently varying the parameters τ and σ , to identify the regimes in the phase diagram. Results of 50 different initial random distributions for $\rho_t(x)$ were averaged. For the mean field model, the system was considered to be inactive whenever $(N(t) - N(t+1))/N(t) < 1 \times 10^{-5}$.

that in the continuous and synchronous regime we must have $z(t) = z_* = [\mu - T_*]/\sqrt{2(\sigma^2 + T_*)}$ and, since $N(t)$ decays precisely like the signal $q(t)$, one can easily derive from equation (2) that $1/\tau = -\log \left[\frac{1}{2} \operatorname{erfc} \left(\frac{\mu - T_*}{\sqrt{2(\sigma^2 + T_*)}} \right) \right]$. However, as $T_* \geq 0$ there is a part of the phase diagram inaccessible in the synchronous regime, given by the following line $\kappa_{\text{na}}(\tau)$ in the $(\kappa, 1/\tau)$ -plane (see SI):

$$\frac{1}{\tau} = -\log \left[\frac{1}{2} \operatorname{erfc} \left(\frac{1}{\sqrt{2\kappa_{\text{na}}}} \right) \right] \quad (4)$$

How well the mean field description captures the microscopic model can be appreciated by comparing Figures 3b and 3c, where we have calculated the cumulative time of inactivity for each model, using Monte Carlo simulations for the microscopic one. Despite the simplicity of equation (2), the agreement with the microscopic model is reasonably good. Notice that these plots show there is a clear border separating the intermittent and synchronous regimes, and that, in general, intermittency can be avoided for faster decays with relatively wide $\rho_t(x)$ distributions, as expected. Furthermore, both models present a gap: below a critical value of $1/\tau$, the system is continuous regardless of how small κ is. The magnitude of this gap is actually a function of μ , and its analytical expression can be found for the mean-field description (see SI). We point out that, unlike the mean-field model, the microscopic one does not present a synchronized regime. Rather, in the latter the activity always lags behind the external signal, *i.e.*, it is always marginally desynchronized. We find, however, that the activity does become less synchronized in the intermittent regime, but no clear transition is observed for this model.

Despite its apparent simplicity, the model presented here is robust enough to be applicable to

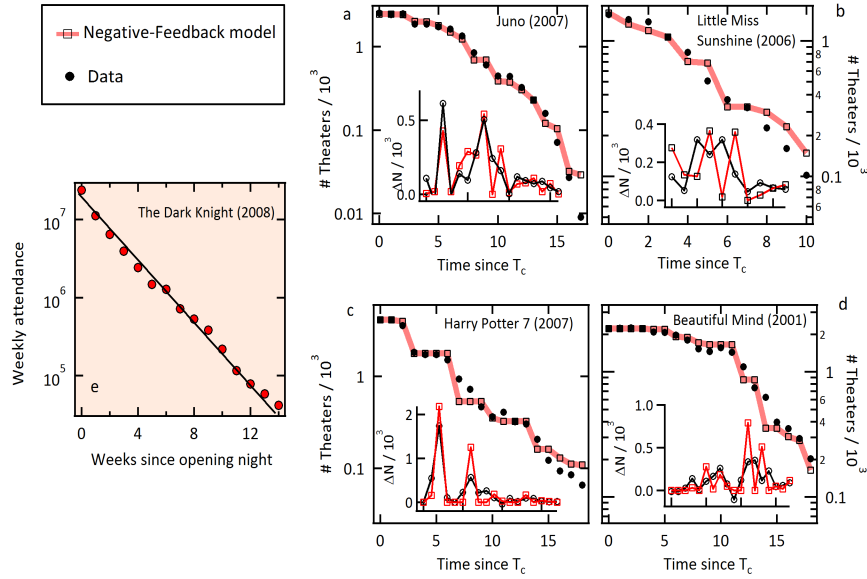


Figure 4: Application of the model to real data. Left plot: Attendance to the movie The Dark Knight (2008). The initial attendance is $q(0) = \$238,615,211 / \7.18 , where \$7.18 is the average ticket price across the U.S. in 2008, evidencing an exponential decay nature of $q(t)$ in this system. Right panel: Negative feedback avalanche examples. Actual (dots) and calculated (squares and thick line) number of theaters vs. time for four different movies. The corresponding insets illustrate the time evolution of the avalanche magnitudes (or activity) ΔN . The parameters used are fixed for all movies ($\mu = 400$, $\sigma = 0.45\mu$), while the average ticket prices employed are \$5.66, \$6.88 and \$7.18 for the years 2001, 2006 and 2007 respectively. T_c is the time in weeks since the maximum attendance was registered, which does not necessarily coincide with the opening week. All data was obtained from www.boxofficemojo.com. See Ref.¹³ for details.

real complex systems. As a proof of principle, we now implement it to investigate the dynamics of the supply of theaters for a given movie that played in the US from 1970 to 2000. The dynamics of the attendance to movie theatres in the U.S. has been studied recently in Ref.¹³, where it was shown that the attendance is in general very well described by a decaying exponential (see example of left plot in Figure 4) as inferred from the weekly revenue of a movie (see SI), and is thus ideally suited to test our model. This system meets our model if we consider that as $q(t)$ people fill up the $N(t)$ theaters at time t , a theater removes the movie at time $t + 1$ if the local attendance $T_i(t)$ is lower than its threshold x_i . In other words, a theater removes a movie after the revenue from one week is below some pre-established value. We assume now that the distribution of local thresholds is again normally distributed. As a first order approximation we assume that at time t the whole available population $q(t)$ is randomly distributed over the available theaters N . We realize that this is an enormous simplification of the actual problem since, of course, geographic restrictions limit the available theaters for people. Nevertheless, similar results as the ones presented below are obtained by sectioning the data and assigning smaller variance per section.

The right panel in Figure 4 presents four examples of how our model (thick pink line and square symbols) is capable of reproducing the theater dynamics (black dots) remarkably well, in some cases spanning almost three orders of magnitude. Note the logarithmic scale on the number of theater axis of this figure. Both small and relatively large events are equally reproducible. In all examples shown, the same parameters $\mu = 400$, $\sigma = 0.45\mu$, were used. In other words, we only require the initial number of theaters to reproduce the whole time series of $N(t)$ using as input the specific time series for $q(t)$ and a normal distribution of thresholds. Other than the fixed choice of

distribution of thresholds, there are no free parameters in this model.

We now apply the model to a collection of 3000 different movies that played in the U.S from 1970 to 2000 (see SI). We postulate that this social system is characterized by a single distribution of thresholds, and therefore, the same parameters $\mu = 400$, $\sigma = 0.45\mu$ are used in all instances, and only $q(t)$ and $N(0)$ are different for each movie and determined by external factors (see SI for further details). To assess the capability of the model to completely recover the dynamics of this social system we obtain the distribution of $\Delta N(t)$ normalized by $N(0)$ for each movie from both the model (solid line in figure 5) and the actual data (dots in figure 5). Notice that the model recovers the whole shape of the distribution of these normalized avalanches. This distribution is actually well fit to a power law with an exponential tail (not shown). In this particular system, an epidemic branching mechanism is responsible for the exponential decay of the effective energy $q(t)$, Ref.¹³. It is possible that other complex systems also present a similar rapid decline of resources, driving the dynamics towards intermittency.

To conclude, we have introduced a negative feedback model with sharp thresholds to describe the dynamics of complex systems driven to extinction, which is simple enough to be amenable to analytical treatment and yet powerful enough to accurately predict the dynamics in real complex systems. We foresee that this model may be used to explain and predict small and large avalanches in other systems for which there is an exponentially fast decline of some quantity playing the role of an energy source randomly distributed among elements that need a certain minimum amount of it to remain active (or survive). Since large avalanches are indeed catastrophic in many social and

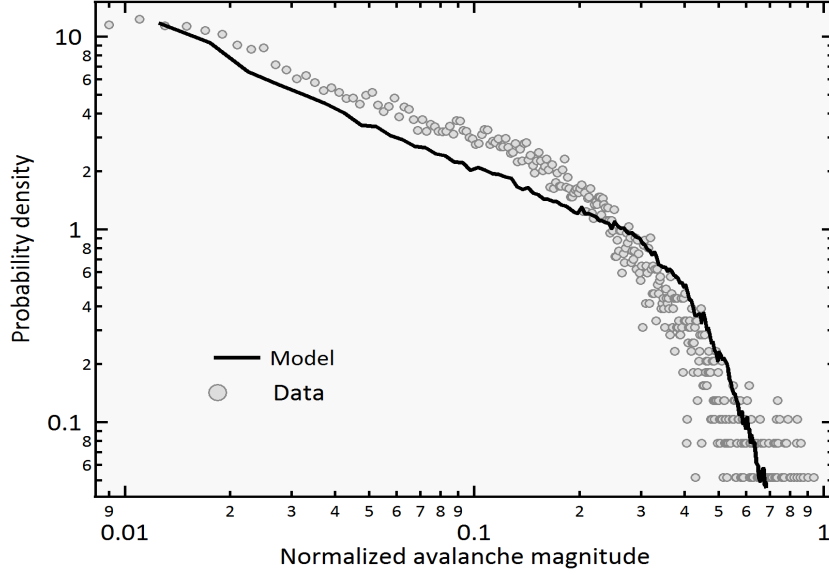


Figure 5: Avalanches in this complex system. Probability density of the avalanche magnitude for the actual data (circles) and for the reproduced data (line) obtained with the microscopic model. Avalanche magnitudes were normalized by the corresponding $N(0)$. A total of 100 runs per movie were averaged to cancel out any special condition of the initial threshold distributions. The distributions $\rho_t(x)$ were chosen randomly from a normal distribution with fixed ($\mu = 400$, $\sigma = 0.45$) for all movies. Note that the model reproduces both small and large events.

natural settings, implementing variations of the model presented in this work could help prevent them.

Supplementary Information is linked to the online version of the paper at www.nature.com/nature

Acknowledgements J. V. E. is grateful to Denis Boyer and Leonardo Dagdug for interesting discussions about the model. J. V. E gratefully acknowledges funds from DGAPA-UNAM No. IA101216 and No. IA103018, as well as from CONACYT No. CB 2013/221235.

Author Contributions J. V. E. proposed the model. I.P.C. solved the model exactly and helped with the analytical understanding. Data and numerical analysis was done by J. V. E. The authors discussed the results and commented the manuscript.

Competing Interests The authors declare that they have no competing financial interests.

Correspondence Correspondence and requests for materials should be addressed to Juan V. Escobar (email: escobar@fisica.unam.mx).

1. P. Bak, C. T. C. & Wiesenfeld, K. Self-organized criticality: an explanation of the $1/f$ noise. *Phys. Rev. Lett.* **59** (1987).
2. Mandelbrot, B. B. & Pignoni, R. *The fractal geometry of nature*, vol. 173 (WH freeman New York, 1983).
3. Dennis, B. Solar hard x-ray bursts. *Solar physics* **100**, 465–490 (1985).

4. Dimiduk, D. M., Woodward, C., LeSar, R. & Uchic, M. D. Scale-free intermittent flow in crystal plasticity. *Science* **312**, 1188–1190 (2006).
5. Barkhausen, H. Zwei mit hilfe der neuen verstärker entdeckte erscheinungen. *Physik Z.* **20**, 401–403 (1919).
6. Raup, D. M. & Sepkoski, J. J. Mass extinctions in the marine fossil record. *Science* **215**, 1501–1503 (1982).
7. Beggs, J. & Plenz, D. Neuronal avalanches in neocortical circuits. *The Journal of Neuroscience* **23**, 11167–11177 (2003).
8. Malamud, B. D., Morein, G. & Turcotte, D. L. Forest fires: an example of self-organized critical behavior. *Science* **281**, 1840–1842 (1998).
9. Malamud, B., Turcotte, D., Guzzetti, F. & Reichenbach, P. Landslide inventories and their statistical properties. *Earth Surface Processes and Landforms* **29**, 687–711 (2004).
10. Huepe, C. & Aldana, M. Intermittency and clustering in a system of self-driven particles. *Physical Review Letters* **92**, 168701 (2004).
11. Manneville, P. *Dissipative structures and weak turbulence* (Academic Press Inc. California, USA, 1990).
12. Adamic, L. A. & Huberman, B. A. The nature of markets in the world wide web. *Quarterly Journal of Electronic Commerce* **512**, 1 (2000).

13. Escobar, J. & Sornette, D. Dynamical signatures of collective quality grading in a social activity: attendance to motion pictures. *Plos One* **10**, 1 (2015).
14. D Sornette, J. B., A Johansen. Stock market crashes, precursors and replicas. *Journal de Physique I* **6**, 167–175 (1996).
15. Sornette D, G. T., Deschatres F & Y, A. Endogenous versus exogenous shocks in complex networks: An empirical test using book sale rankings. *Phys. Rev. Lett.* **93**, 228701 (2004).
16. Sornette, D. *Critical Phenomena in Natural Sciences* (Springer, Heidelberg, 2nd edition, 2003).
17. Stanley, H. Scaling, universality, and renormalization: Three pillars of modern critical phenomena. *Rev. Mod. Phys.* **71**, S358 (1999).
18. Bak, P. & Tang, C. Earthquakes as a self-organized critical phenomenon. *Journal Of Geophysical Research*, **94** (1989).
19. A. Sornette, D. S. Self-organized criticality and earthquakes. *Europhysics Letters* **9**, 197 (1989).
20. Z. Olami, H. F. & Christensen, K. Self-organized criticality in a continuous, nonconservative cellular automaton modeling earthquakes. *Phys. Rev. Lett.* **68**, 1244 (1992).
21. P. Bak, C. T. & Wiesenfeld, K. Self organized criticality. *Phys. Rev. A* **38**, 364 (1988).
22. Fischer, R., Gondret, P. & Rabaud, M. Transition by intermittency in granular matter: from discontinuous avalanches to continuous flow. *Phys. Rev. Lett.* **103**, 128002 (2009).

23. Martin, P. C., Siggia, E. D. & Rose, H. A. Statistical dynamics of classical systems. *Phys. Rev. A* **8**, 423–437 (1973).

Supplemental Information

Analytical treatment of the model

In this section we show the derivation of a naïve mean field solution for the dynamics. Based on this result we perform a bifurcation type analysis to obtain the line separating the synchronous regime to the asynchronous one,

A naïve dynamical mean-field equation.

As explained in the main text the microscopic dynamics is given by

$$\sigma_i(t+1) = \sigma_i(t)\Theta(T_i(t) - x_i) , \quad (5)$$

with $N(t) = \sum_{i=1}^N \sigma_i(t)$ and $\sigma_i(t) \in \{0, 1\}$ and $q(t) = \sum_{i=1}^{N(t)} T_i(t)$. The probability of finding the local attendances at a given configuration $\{T_i(t)\}$ is a multinomial distribution with uniform distribution $1/N(t)$, that is:

$$\text{Prob}(\{T_i(t)\}) = \frac{q(t)!}{\prod_{i=1}^{N(t)} q_i(t)!} \left(\frac{1}{N(t)} \right)^{q(t)} . \quad (6)$$

Thus, the first two cumulants of $T_i(t)$ are $E[T_i(t)] = q(t)/N(t)$ and $\text{Var}[T_i(t)] = q(t)[N(t) - 1]/N^2(t) \simeq q(t)/N(t)$, respectively. Moreover the covariance is $\text{Cov}[T_i(t), T_j(t)] = -q(t)/N^2(t)$,

which implies that for large $N(t)$ the variables are weakly correlated. This suggests to reasonably assume the occupancies $\{T_i(t)\}$ to be i.i.d random Gaussian variables as follows :

$$T_i(t) = \frac{q(t)}{N(t)} + \sqrt{\frac{q(t)}{N(t)}} \zeta_i(t), \quad (7)$$

with $\zeta_i(t) \sim \mathcal{N}(0, 1)$. Since the occupancies are definite positive, one can introduce a cut-off in the Gaussian distribution to ensure that $T_i(t) \geq 0$, However this only affects the dynamics at the late stages, so one can simply ignore it for the sake of simplicity. Similarly, we assume that the distribution of thresholds follows a Gaussian distribution (same argument for a possible cut-off) with mean value μ and variance σ^2 , or in other words: $x_i = \mu + \sigma \xi_i(t)$ with $\xi_i(t) \sim \mathcal{N}(0, 1)$.

Then, starting from the microscopic dynamical equation (5), we try to write a corresponding closed evolution equation for the variable $N(t) = \sum_{i=1}^N \sigma_i(t)$ neglecting time and space fluctuations (a naïve mean field approximation), viz.

$$\begin{aligned} N(t+1) &= \sum_{i=1}^N \sigma_i(t) \Theta \left(\frac{q(t)}{N(t)} + \sqrt{\frac{q(t)}{N(t)}} \zeta_i(t) - \mu - \sigma \xi_i(t) \right) \\ &\approx N(t) \left\langle \Theta \left(\frac{q(t)}{N(t)} + \sqrt{\frac{q(t)}{N(t)}} \zeta(t) - \mu - \sigma \xi \right) \right\rangle_{(\zeta, \xi)} \\ &= N(t) \int dx \Theta \left(\frac{q(t)}{n(t)} - \mu + x \right) \rho(x|N(t)), \end{aligned}$$

where we have defined

$$\rho(x|N(t)) \equiv \left\langle \delta \left(x - \sqrt{\frac{q(t)}{N(t)}} \zeta + \sigma \xi \right) \right\rangle_{(\zeta, \xi)} = \sqrt{\frac{1}{2\pi \left(\frac{q(t)}{n(t)} + \sigma^2 \right)}} \exp \left[-\frac{x^2}{2 \left(\frac{q(t)}{N(t)} + \sigma^2 \right)} \right].$$

This, in turn, implies that:

$$N(t+1) = \frac{N(t)}{2} \left[\operatorname{erfc} \left(\frac{\mu - \frac{q(t)}{N(t)}}{\sqrt{2 \left(\frac{q(t)}{N(t)} + \sigma^2 \right)}} \right) \right].$$

Bifurcation analysis.

A quick look at the naïve dynamical mean-field equation suggests that we should expect two types of regimes in the parameter space: one in which the system is able to keep up with the external signal (the continuous & synchronous regime) and another one in which it does not (the continuous & asynchronous regime I) .

In order to identify this transition, we consider an exponentially decaying external signal $q(t) = q(0)e^{-t/\tau}$ henceforth. Let us first define $z(t) = \frac{\mu - T(t)}{\sqrt{2(\sigma^2 + T(t))}}$. If $z(t)$ were to be a constant, $z(t) = z_*$, then, according to equation (8) we must have that $N(t) = N(0) \left(\frac{\text{erfc}(z_*)}{2} \right)^t = N(0) \left[\frac{\text{erfc}(z_*)}{2} \right]^t \equiv N(0) \exp[-t/\tau_n]$, where we have defined $\frac{1}{\tau_n} \equiv -\log \left[\frac{\text{erfc}(z_*)}{2} \right]$. On the other hand, since we are requiring $z_* = z(t) = \frac{\mu - T(t)}{\sqrt{2(\sigma^2 + T(t))}}$ this automatically implies, as a matter of consistency, that $\tau = \tau_n$. Thus, for the region of the parameter space in which this identity holds, $N(t)$ and $q(t)$ do synchronize, and there are no avalanches. To identify in which part of the phase diagram a change of regime occur, we assume a continuous bifurcation to the region in which $\tau \neq \tau_n$. After some algebra we have the following set of coupled equations:

$$\begin{cases} e^{z_*^2} \text{erfc}(z_*) = \frac{(\mu + 2(\kappa\mu)^2 + T_*)T_*}{2\sqrt{2\pi}((\kappa\mu)^2 + T_*)^{3/2}} \\ z_*(\tau) = \frac{\mu - T_*}{\sqrt{2((\kappa\mu)^2 + T_*)}} \end{cases}, \quad (8)$$

with $\frac{1}{\tau} = -\log \left[\frac{\text{erfc}(z_*)}{2} \right]$. Given μ , the solution of (8) results in a pair $(\kappa_c(\tau), T_*(\tau))$. The first function $\kappa_c(\tau)$ corresponds to the bifurcation line separating both regimes. The line $T_*(\tau)$ tells which value $T(t)$ takes precisely at the transition.

To check the validity of these results, we have simulated numerically eq. (8) and use the following parameter as a proxy for identifying the transition from the synchronous to the asynchronous

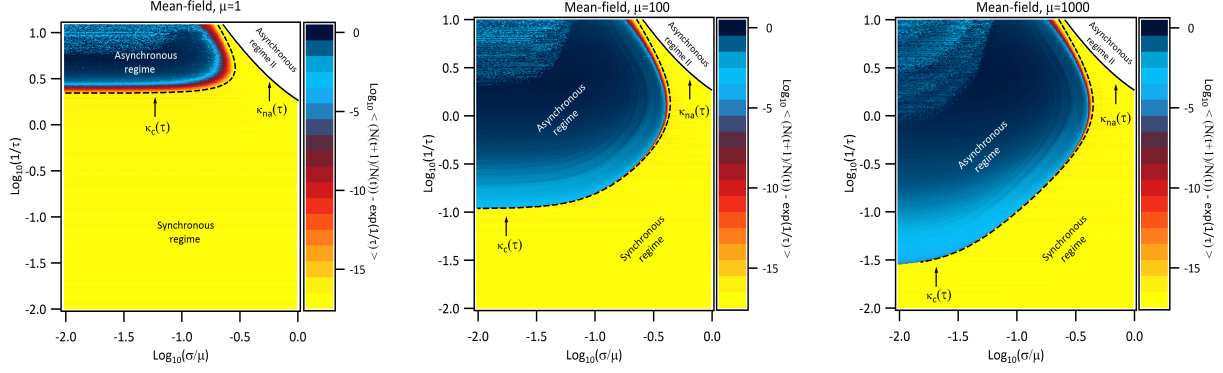


Figure 6: Phase diagram for the mean-field equation (8) for $\mu = 1$ (left), $\mu = 100$ (center) and $\mu = 1000$ (right).

regime:

$$\mathcal{O} = \lim_{T \rightarrow \infty} \frac{1}{T} \sum_{t=1}^T \left| \frac{n(t+1)}{n(t)} - e^{-\frac{1}{\tau}} \right| \quad (9)$$

This parameter has two drawbacks: First of all, it assumes a finite number of steps for the system to reach a quasi-stationary state, and secondly, it assumes that we can take a large enough time window. Clearly, these two assumptions will not be met when doing simulations. However, we can numerically compensate this when trying to identify the transition line by taking $\mathcal{O} < \epsilon$, for moderate values of ϵ . The corresponding line should be a lower bound of the analytical solution. A comparison between theory (dashed lines) and simulations is summarised in Figure 6 for three values of $\mu = 1$, $\mu = 100$ and $\mu = 1000$. Some comments are in order. First of all, we see that the comparison between the theory (8) and simulations is fairly good. Second of all, we note that, given a value of μ , there exists a value of τ , denoted τ_{gap} , below which there only exists the continuous regime. To find τ_{gap} as a function of μ , we simply put $\kappa = 0$ and solve the corresponding equations

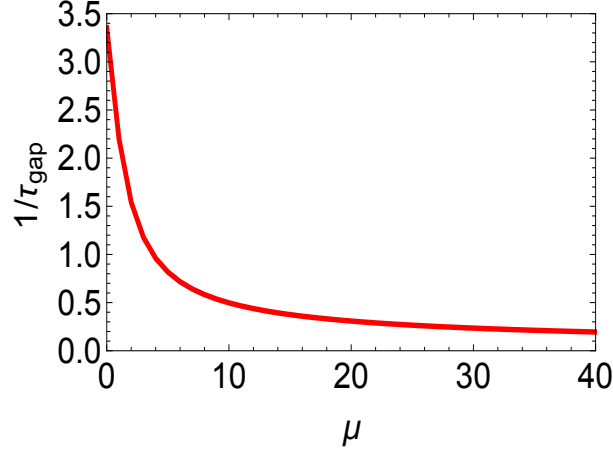


Figure 7: Left: Plot of $1/\tau_{\text{gap}}$ as function of μ .

(8), obtaining:

$$\mu = -\frac{z_{\star}^2(\tau_{\text{gap}})}{2} + 2\pi e^{2z_{\star}^2(\tau_{\text{gap}})} \text{erfc}^2[z_{\star}(\tau_{\text{gap}})] . \quad (10)$$

This also implies that as $\mu \geq 0$, the gap has a maximum given by the solution:

$$z_{\star}(\tau_{\text{gap}}^{(\max)}) = 2\sqrt{\pi} e^{z_{\star}^2(\tau_{\text{gap}}^{(\max)})} \text{erfc}[z_{\star}(\tau_{\text{gap}}^{(\max)})] , \quad (11)$$

which yields $1/\tau_{\text{gap}}^{(\max)} = 3.35229 \dots$. A plot of the gap as a function of μ can be found in Figure

7. Actually in the limit $\mu \rightarrow \infty$ we bifurcation line $\kappa_c(\tau)$ takes the following simpler form:

$$\kappa(\tau) = \frac{1}{\sqrt{2}} \frac{1}{\sqrt{\pi} e^{z_{\star}^2(\tau)} \text{erfc}(z_{\star}(\tau)) + z_{\star}(\tau)} . \quad (12)$$

As it turns out, there exists another region in the parameter space in which the system is not able to synchronize with the external signal, but this is due solely to the impossibility of the system to satisfy the conditions of the model. Indeed, notice that τ is an external parameter, while τ_n is given in terms of z_{\star} , that, in turn, depends on the value T_{\star} . This means that there exists a region in the parameter space in which $\tau \neq \tau_n$ as there is no initial conditions that will allow the system to

realise $\tau = \tau_n$ after some transient. More precisely, we notice that:

$$\frac{1}{\tau} = -\log \left[\frac{1}{2} \operatorname{erfc} \left(\frac{1 - T_*/\mu}{\sqrt{2(\kappa^2 + T_*/\mu^2)}} \right) \right] \leq -\log \left[\frac{1}{2} \operatorname{erfc} \left(\frac{1}{\sqrt{2}\kappa} \right) \right] \equiv \frac{1}{\tau_{\text{na}}}, \quad (13)$$

where we have used the fact that T_* and μ are both non-negative (at least in the context in which the model has been introduced). This naturally implies that above the bound $1/\tau_{\text{na}}$ the corresponding region in the parameter space cannot realize the condition $\tau = \tau_n$ and $N(t)$ must decay more slowly than the external signal. This is what we call the continuous & asynchronous regime II. In the $(\kappa, 1/\tau)$ -plane, the line $\kappa_{\text{na}}(\tau)$ separating this region is thus given by:

$$-\log \left[\frac{1}{2} \operatorname{erfc} \left(\frac{1}{\sqrt{2}\kappa_{\text{na}}} \right) \right] = \frac{1}{\tau}, \quad (14)$$

which is shown in Figure 6, as well as in Figure 3a on the main text.

Phase diagram of microscopic model

As explained in the main text, to obtain the correct phase diagram we used Monte Carlo simulations of the microscopic dynamical equation (5) to identify the various phases in the parameter space $(\kappa, 1/\tau)$. As a proxy of inactivity over time, we have used the normalized cumulative time of inactivity. This is calculated by adding up the intervals Δt during which the activity remained unchanged, and subsequently dividing by the total duration of the activity, t_{TOTAL} . We consider the activity to last for a number $t_{\text{TOTAL}} = t_f - t_i$ of iterations, where t_i is the first iteration for which $N(t_i + 1) \neq N(t_i)$, and t_f is the first iteration for which either $N(t_f) < 10$ or $T(t_f) < 10$. Figure 8 shows an example of the use of this metric for a particular time series.

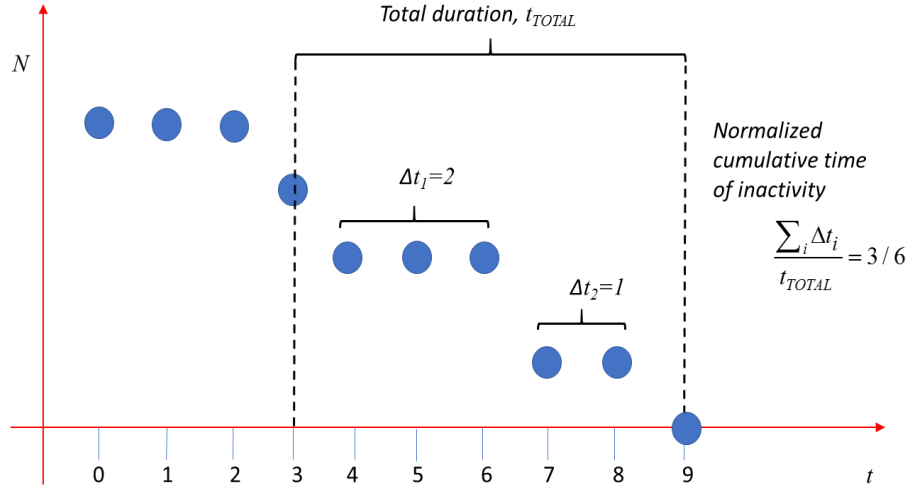


Figure 8: Pictorial representation to estimate the normalized cumulative time of inactivity.

Data analysis: comparison with real data

A data set consisting of both the time series for the weekly revenue and number of theaters of over 10,000 different movies was obtained from the website www.boxofficemojo.com. We kept only those 3469 that played in the U.S.A. for at least four consecutive weeks in no less than 50 theaters. The fit of the gross income to an exponential was in general excellent, with 90% of the correlation coefficients being higher than 0.98. An algorithm designed to fit noisy data was implemented that is able to signal when a change of dynamics has taken place so that only the portion of a given time series corresponding to the exponential decay was taken into account for the analysis. To obtain the number of people $q(t)$ that attended on a given week, the gross income per week for that movie was divided by the average ticket price for that year. The microscopic simulations were implementing using as initial conditions those found on the critical week t_c ,

defined as the latest week on which the movie was played in the maximum number of theaters. The reasoning behind this is the realization that new theaters will act as sources of exogenous shocks, which act as sources of new audience and may hinder the exponential relaxation of $q(t)$. Therefore, we expect that the system will relax without any further input once the number of theaters showing the movies does not increase anymore. Simulations of the microscopic model were performed for each movie using $q(0) = q(t_c)$ and $N(0) = N(t_c)$. Avalanche magnitudes, $N(t - 1) - N(t)$ at every iteration t were normalized by the corresponding $N(0)$. The distribution obtained for the microscopic simulations were averaged from 100 different initial thresholds distributions for each time series. Further details about the algorithm mentioned above as well as about the fitting procedure and results can be found in reference¹³.